

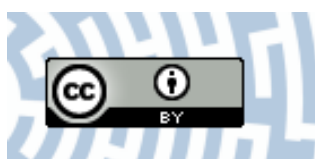


You have downloaded a document from  
**RE-BUŚ**  
repository of the University of Silesia in Katowice

**Title:** Technogenic magnetic particles in alkaline dusts from power and cement plants

**Author:** Tadeusz Magiera, Beata Gołuchowska, Mariola Jabłońska

**Citation style:** Magiera Tadeusz, Gołuchowska Beata, Jabłońska Mariola. (2013). Technogenic magnetic particles in alkaline dusts from power and cement plants. "Water, Air, and Soil Pollution" (Vol. 224, no. 1 (2013), art. no. 1389), doi 10.1007/s11270-012-1389-9



Uznanie autorstwa - Licencja ta pozwala na kopiowanie, zmienianie, rozprowadzanie, przedstawianie i wykonywanie utworu jedynie pod warunkiem oznaczenia autorstwa.



# Technogenic Magnetic Particles in Alkaline Dusts from Power and Cement Plants

Tadeusz Magiera · Beata Gołuchowska · Mariola Jabłońska

Received: 4 September 2012 / Accepted: 7 November 2012 / Published online: 27 November 2012  
© The Author(s) 2012. This article is published with open access at Springerlink.com

**Abstract** During this study, we investigated the mineralogical characterization of technogenic magnetic particles (TMPs) contained in alkaline industrial dust and fly ash emitted by coal burning power plants and cement plants. The reaction of tested dust samples varied between values of pH 8 and pH 12. Their magnetic properties were characterized by measurement of magnetic susceptibility ( $\chi$ ), frequency dependence of magnetic susceptibility ( $\chi_{fd}$ ), and temperature dependence of magnetic susceptibility. Mineralogical and geochemical analyses included scanning electron microscopy with energy dispersive spectroscopy, microprobe analysis and X-ray diffraction. The TMPs in fly ash from hard coal combustion have the form of typical magnetic spherules with a smooth or corrugated surface as well as a skeletal morphology, composed of iron oxides (magnetite, maghemite, and magnesioferrite) that occurred in the form of incrustation on the

surface of mullite, amorphous silica, or aluminosilicate particles. The TMPs observed in fly ash from lignite combustion have a similar morphological form but a different mineralogical composition. Instead of magnetite and magnesioferrite, maghemite and hematite with lower  $\chi$  values were the prevailing magnetic minerals, which explains the much lower magnetic susceptibility of this kind of ash in comparison with the ash from hard coal combustion, and probably results from the lower temperature of lignite combustion. Morphology and mineralogical composition of TMPs in cement dust is more diverse. The magnetic fraction of cement dust occurs mostly in the form of angular and octahedral grains of a significantly finer granulation ( $<20 \mu\text{m}$ ); however, spherules are also present. A very characteristic magnetic form for cement dust is calcium ferrite ( $\text{CaFe}_3\text{O}_5$ ). The greatest impact on the magnetic susceptibility of cement dust results from iron-bearing additives (often waste materials from other branches of industry), which should be considered the most dangerous to the environment. Stoichiometric analysis of micro-particles confirmed the presence of heavy metals such as Pb, Mn, Cd, and Zn connected with TMPs, which are carriers of magnetic signals in atmospheric dust. Therefore, in some cases, their presence in topsoil when detected by magnetic measurement can be treated as an indicator of inorganic soil contamination.

---

T. Magiera (✉) · B. Gołuchowska  
Department of Land Protection,  
University of Opole, Opole, Poland  
e-mail: tmagiera@ipis.zabrze.pl

T. Magiera  
Institute of Environmental Engineering,  
Polish Academy of Sciences, Zabrze, Poland

M. Jabłońska  
Department of Geochemistry, Mineralogy and  
Petrology, Faculty of Earth Sciences,  
University of Silesia, Sosnowiec, Poland

**Keywords** Alkaline dusts · Magnetic susceptibility · Technogenic magnetic particles · Iron mineralogy

## 1 Introduction

The wide use of coal as an energy source, combined with the intensive development of many branches of industry, including chemical, ceramic, and cement production at the beginning of the twentieth century, has resulted in the emission into the atmosphere of extremely large amounts of industrial dust and fly ash. This dust usually has an alkaline reaction ( $\text{pH} > 7.2$ ) and contains a significant amount of trace elements, constituting a potential threat to the natural environment and living organisms. Dust particles deposited on the soil surface, in contact with the acidic soil environment, especially in forest areas, may cause the release of potentially toxic trace elements that create a threat to the environment (Strzyszczyński and Magiera 1998; Klose et al. 2001; Polat et al. 2004).

Alkaline dust is also deposited directly on the surface of plants. Taking into account that the size of the stoma in stomata apparatus varies from 8 to 10  $\mu\text{m}$ , dust particles with a diameter similar to that of the stoma can block its aperture. However, smaller particles can penetrate directly into leaf tissue. Despite the fact that the leaves of most plants are protected by cuticle, this protective layer can be dissolved by alkaline dust, especially cement and lime dust which contains large amounts of calcium oxide. It has been proven that pine bark, with a pH of between 3 and 4, can be substantially damaged during contact with aggressive alkaline dust of a pH higher than 10 (Farmer 1993; Migaszewski et al. 2001).

Much more hazardous to the environment are heavy metals contained in alkaline dust. Heavy metals in fly ash originate from the mineral content of coal and—during its combustion—move from the furnace, through the slag traps, de-dusting devices, and up the chimney. The presence of heavy metals (Be, Cr, Zn, Co, Mo, Ni, Pb, and Ti) in various grain fractions of fly ash from Polish power plants, and the close relationship between metal content in ash and the specific surface area of its particles, has been frequently observed (Koniecznyński and Żeliński 2009). A very high risk to the environment is posed by fine dust fraction. Fe-rich, magnetic particles found in atmospheric dust in Rome were mostly 0.1–5  $\mu\text{m}$  in size (Sagnotti et al. 2009). This fraction is characterized by the greatest content of metals and the least effective retention by electrostatic precipitators. Geochemical analysis has shown that the content of trace elements such as Zn,

Ga, Cd, Cu, Mo, Pb, and Tl, known as easily volatile, increases with the increase in the degree of fineness of ash particles. This occurs as a result of vaporization of these elements during coal combustion, followed by deposition and surface condensation on ash grains after lowering the ambient temperature (Koniecznyński et al. 2007; Koniecznyński and Stec 2009).

The degree of potential toxicity of heavy metals depends on the form of binding with the mineral phase. Research by Hullet et al. (1980), and also later other authors (Hansen et al. 1981; Vassilev et al. 2001, 2004) show that most of the elements belonging to the first and second transition series, such as Pb, Zn, Cd, V, Cr, Co, Ni, and Cu, occurring in coal mainly in the form of sulfides, are bound with magnetic minerals in fly ash. The crystallographic structure of magnetite and various ferrites formed at high temperatures allows for the introduction of numerous elements into fly ash, which can be potentially hazardous for plants, animals, and humans in the soil environment. Geochemical studies of fly ash have proven that heavy metals can also be adsorbed on a particle's surface (Vaughan et al. 2002; Giere and Querol 2010). In particular, the finest fraction of fly ash, with a highly developed specific surface area, may be enriched in such metals as Cr, Mn, Pb, V, and Zn (Keyser et al. 1978). Heavy metals that are only connected to the surface of ash particles by adsorption forces are easily activated in the soil under the influence of organic acids and pose a serious hazard to the biological environment. The progressive acidification of soils associated with emissions of  $\text{SO}_2$  and then deposition in the form of acid rain accelerates the release of heavy metals.

By the 1980s, many researchers had already noted the relationship between increase in magnetic susceptibility and the content of heavy metals in many environments. Hunt et al. (1984) show a linear correlation between the content of magnetic particles in urban dust and the content of such metals as Pb, Cu, Zn, and Cd. A similar correlation between magnetic susceptibility and the content of Cu, Fe, Pb, and Zn in atmospheric dust is observed by Beckwith et al. (1986). The presence of magnetic particles was also found in cement dust (Strzyszczyński 1995; Gołuchowska 2001). In this case, the main source of magnetic particles and associated heavy metals are additives and fuels used in the process of clinker burning. These additives are often waste materials from other

branches of industry, such as metallurgical waste, cinder pyrites, fly ash etc.

The research presented in this work aimed at carrying out a detailed description of mineralogical characteristics and morphology of the mineral particles of alkaline dust from power stations and cement plants of southern Poland, with special regard to the magnetic phase of this dust as the main carrier of heavy metals. This phase, easily detectable by geophysical measurements, can be used as an indicator supporting quantitative evaluation of the content of potentially toxic metals in the environment.

## 2 Materials and Methods

In this study, 15 samples of fly ash were examined; of which ten came from nine Polish power plants burning hard coal, and five from lignite burning power plants. In addition, 12 samples of cement and lime dust arising from plants located in the province of Opole (Southern Poland) were tested. Fly ash was collected from different areas of electrofilters. Cement dust was taken both from electrofilters and from the dustfall in the vicinity of cement plants.

The first step of the study was to take measurements of low-frequency magnetic susceptibility ( $\kappa$ ) in the laboratory using an MS2 “Bartington” magnetic susceptibility meter and MS2B sensor. The result of the measurements obtained for a dust sample of a certain density was converted to mass magnetic susceptibility ( $\chi$ ) and expressed as cubic meters per kilogram (Thompson and Oldfield 1986).

To determine frequency-dependent magnetic susceptibility ( $\chi_{fd}$ ), additional measurements at high frequency (4,700 Hz) were carried out. Frequency-dependent magnetic susceptibility is a parameter that helps to determine the presence of superparamagnetic fraction in the tested sample, i.e., magnetic particles  $<0.02 \mu\text{m}$ . The  $\chi_{fd}$  parameter is expressed in percentages and calculated by the formula:

$$\chi_{fd} = \chi_{LF} - \chi_{HF} / \chi_{LF} \cdot 100\%$$

where:

- $\chi_{fd}$  Frequency-dependent magnetic susceptibility
- $\chi_{LF}$  Magnetic susceptibility measured in low magnetic field at a frequency of 470 Hz
- $\chi_{HF}$  Magnetic susceptibility measured in low magnetic field at a frequency of 4,700 Hz.

In the second stage, pH measurements of the tested dust samples were undertaken in distilled water by means of the potentiometric method using a pH-meter N-5170 TELEKO and a complex electrode ESAgP-309W EUROSENSOR. The pH meter was calibrated using buffer solutions of pH 7 and pH 9. Measurements were performed after 3 h following the preparation of the suspension of 1:2.5 (w/v) dust/water.

In the next stage of research, samples were subjected to mineralogical and chemical analysis by the application of the scanning electron microscopy (SEM) technique, together with energy dispersive spectrometry (EDS). The SEM analysis was performed using an environmental scanning electron microscope Philips XL 30 ESEM/TMP with an analytic EDS unit (EDAX detector, Sapphire type). A primary beam with an accelerating voltage of 15 keV was applied. Using this analytical method, images recording both morphology and size of magnetic particles separated from the dust samples were obtained. Additionally, the chemical micro-analysis with the use of a CAMECA SX100 electron microprobe was conducted on selected samples. For SEM and microprobe analysis the TMPs (technogenic magnetic particles) fraction was enriched by magnetic separation. The separation was held in isopropanol, using an ultrasonic washer, which simplified the separation of individual grains.

Samples were also subjected to mineralogical analysis using the X-ray diffraction technique by powder method. Mineralogical composition of the samples was determined by means of standards, using a Philips PW 3710 X-ray diffractometer and X'PERT computer program. In the X-ray analysis, the Rietveld method was applied to quantify the contribution of each phase to the examined magnetic concentrates.

The selected samples were subjected to thermomagnetic analysis. Measurements were performed using the AGICO KLY-4S susceptibility bridge, equipped with a CS-3 heating chamber, employing a temperature range from room temperature to 700 °C, in ambient air, with a heating rate of 8.5 °C/min.

## 3 Results

Magnetic susceptibility of different kinds of industrial dust is considerably variable, but is generally very

high. Compared with other types of analyzed industrial dust, fly ash originating from hard coal burning is characterized by the highest value of magnetic susceptibility. The average values of  $\chi$  obtained for ten ash samples from nine Polish power plants burning hard coal and thermal power stations in all cases exceed a value of  $1,000 \times 10^{-8} \text{ m}^3 \text{ kg}^{-1}$ , reaching the value of  $8,500 \times 10^{-8} \text{ m}^3 \text{ kg}^{-1}$  (Table 1). These values not only depend on the origin of burned coal and the total content of iron in coal, but also on combustion conditions.

A characteristic feature of all fly ash samples from hard coal burning is the low value of frequency-dependent magnetic susceptibility ( $\chi_{fd}$ ). This parameter did not exceed the value of 4 % in any of the tested samples. Such low values of  $\chi_{fd}$  means an almost total

absence of superparamagnetic grains (magnetic particles  $< 0.02 \mu\text{m}$ ) within the magnetic fraction. This is a factor which allows ferrimagnetic grains of anthropogenic origin, originating from fly ash fallout that usually occurs as a multidomain size, to be distinguished from natural ferrimagnetic grains of biogenic origin (produced by magnetotactic bacteria), or from pedogenic grains formed as a result of precipitation of iron minerals from soil solutions. This parameter is therefore helpful in detecting the presence of industrial dust in the topsoil.

Fly ash originating from lignite combustion has lower  $\chi$  values. In five tested samples the values ranged between 548 and  $590 \times 10^{-8} \text{ m}^3 \text{ kg}^{-1}$ . The  $\chi_{fd}$  parameter reached a maximum value of 1.5 % (Table 1).

**Table 1** Magnetic susceptibility,  $\chi$ , frequency-dependent magnetic susceptibility,  $\chi_{fd}$ , and pH of fly ash, cement, and lime dust samples

Sample no.	Description	$\chi$ ( $\times 10^{-8} \text{ m}^3 \text{ kg}^{-1}$ )	$\chi_{fd}$ (%)	pH
1.	Dust from hard coal combustion	7,428	2.9	8.8
2.	Dust from hard coal combustion	2,588	1.2	9.0
3.	Dust from hard coal combustion	5,049	1.0	9.0
4.	Dust from hard coal combustion	8,516	2.1	9.2
5.	Dust from hard coal combustion	7,941	2.8	9.9
6.	Dust from hard coal combustion	1,691	1.1	10.0
7.	Dust from hard coal combustion	5,650	2.2	9.1
8.	Dust from hard coal combustion	3,776	3.6	10.3
9.	Dust from hard coal combustion	7,364	0.9	9.3
10.	Dust from hard coal combustion	4,102	3.5	9.4
11.	Dust from lignite combustion	590	1.3	8.8
12.	Dust from lignite combustion	552	1.0	9.2
13.	Dust from lignite combustion	552	0.7	9.4
14.	Dust from lignite combustion	582	1.5	8.5
15.	Dust from lignite combustion	548	0.1	8.4
16.	Cement dust—first section of electrostatic precipitator	82	5.4	8.4
17.	Cement dust—second section of electrostatic precipitator	66	4.2	8.8
18.	Cement dust—behind electrostatic precipitator	806	2.2	9.2
19.	Cement dust—behind electrostatic precipitator	97	2.1	11.9
20.	Cement dust—dustfall	233	1.9	7.9
21.	Cement dust—first section of electrostatic precipitator	199	1.9	8.2
22.	Cement dust—second section of electrostatic precipitator	101	2.7	9.4
23.	Cement dust—behind electrostatic precipitator	142	2.1	8.6
24.	Lime plant—chimney	5	—	11.9
25.	Lime plant—chimney electrostatic precipitator	3	—	7.0
26.	Lime plant—worm	2	—	11.5
27.	Lime plant—worm electrostatic precipitator	1	—	8.0



The average  $\chi$  values for cement and lime dust varied in a very wide range from  $1 \times 10^{-8} \text{ m}^3 \text{ kg}^{-1}$  to more than  $800 \times 10^{-8} \text{ m}^3 \text{ kg}^{-1}$  (Table 1). The lowest  $\chi$  values are characteristic of paramagnetic minerals and reveal a complete lack of ferrimagnetic iron oxides in the mineralogical composition of this dust. Such a wide variation is caused by the various additives used during cement production. These materials are often iron-bearing wastes from metallurgy, power plants, ore processing etc. Metallurgical wastes and fly ashes from hard coal combustion are of the greatest importance in the process of magnetic enrichment of cement dust (Gołuchowska 2001).

Almost all tested samples were characterized by pH values greater than 8.0, and so were alkaline.

Observations of fly ash particles from the combustion of hard coal with SEM technique showed that a

significant share, both in magnetic and silicate phases, have spherical forms of various sizes from several to dozens of micrometers, called magnetic spherules (Puffer et al. 1980). Some have a smooth surface, and others a corrugated or even skeletal morphology. Magnetic iron oxides frequently occur in the form of incrustation on the surface of mullite, amorphous silica, or aluminosilicate. Other spherules consist entirely of a ferrimagnetic shell built of iron oxide (magnetite and maghemite), and their inside is void with visible holes after the exit of the gas which originally filled the spherules (Fig. 1a).

The components of fly ash also include aluminosilicate particles occurring frequently in oval or spherical forms, usually with a smooth surface. Angular forms were rarely observed. The forms of spherical or near-

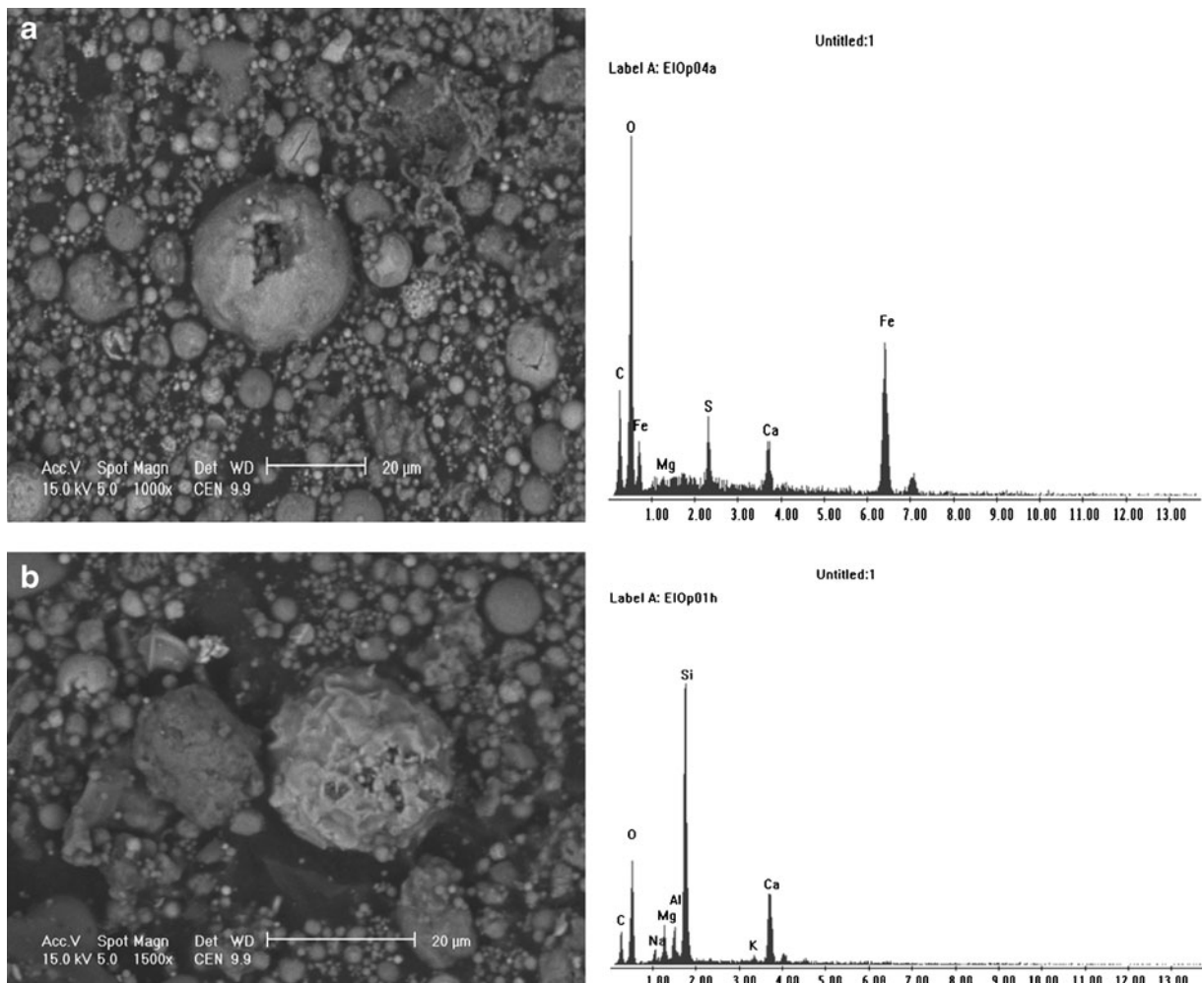


**Fig. 1** SEM micrographs of fly ash from hard coal burning power plant with EDS spectra: **a** accumulation of hollow particles with iron oxide composition, **b** quartz particle

spherical aluminosilicates are typical of coal combustion processes. Silica ( $\text{SiO}_2$ ) present in fly ash occurs in crystalline form (quartz and mullite) as well as in a glassy phase form. Particles of quartz were observed in the form of spherical and angular grains of 10 to 18  $\mu\text{m}$  diameter (Fig. 1b), containing admixtures of magnesium, aluminum, and calcium. Calcite ( $\text{CaCO}_3$ ) particles were also observed in the form of angular grains with smooth surfaces, with a size not exceeding 10  $\mu\text{m}$ .

Morphological forms of minerals occurring in ash originating from the combustion of lignite did not differ from the forms of those with an origin in the combustion of hard coal. In samples of fly ash formed after lignite combustion, aluminosilicate particles occurring with the elements barium, potassium, mag-

nesium, and iron were frequently identified. These took spherical forms with smooth surfaces with a size not exceeding 50  $\mu\text{m}$ . The spherules were varied, from forms with completely smooth surfaces to forms with extensive corrugated surfaces. Forms with incrustation of iron oxides (probably hematite) on the silicate core of magnetic spherules were also found (Fig. 2a). The magnetic fraction was also present in the form of angular grains (Fig. 2b). Cross-sections of magnetic particles observed with the microprobe showed that they have a contrast phase composition built of both non-stoichiometric iron oxides of maghemite–magnetite series and hematite coexisting with siliceous glaze, mullite, or other forms of silica and aluminosilicates (Fig. 3, Table 2). The metal oxides were often present in the form of incrustations, and some formed empty

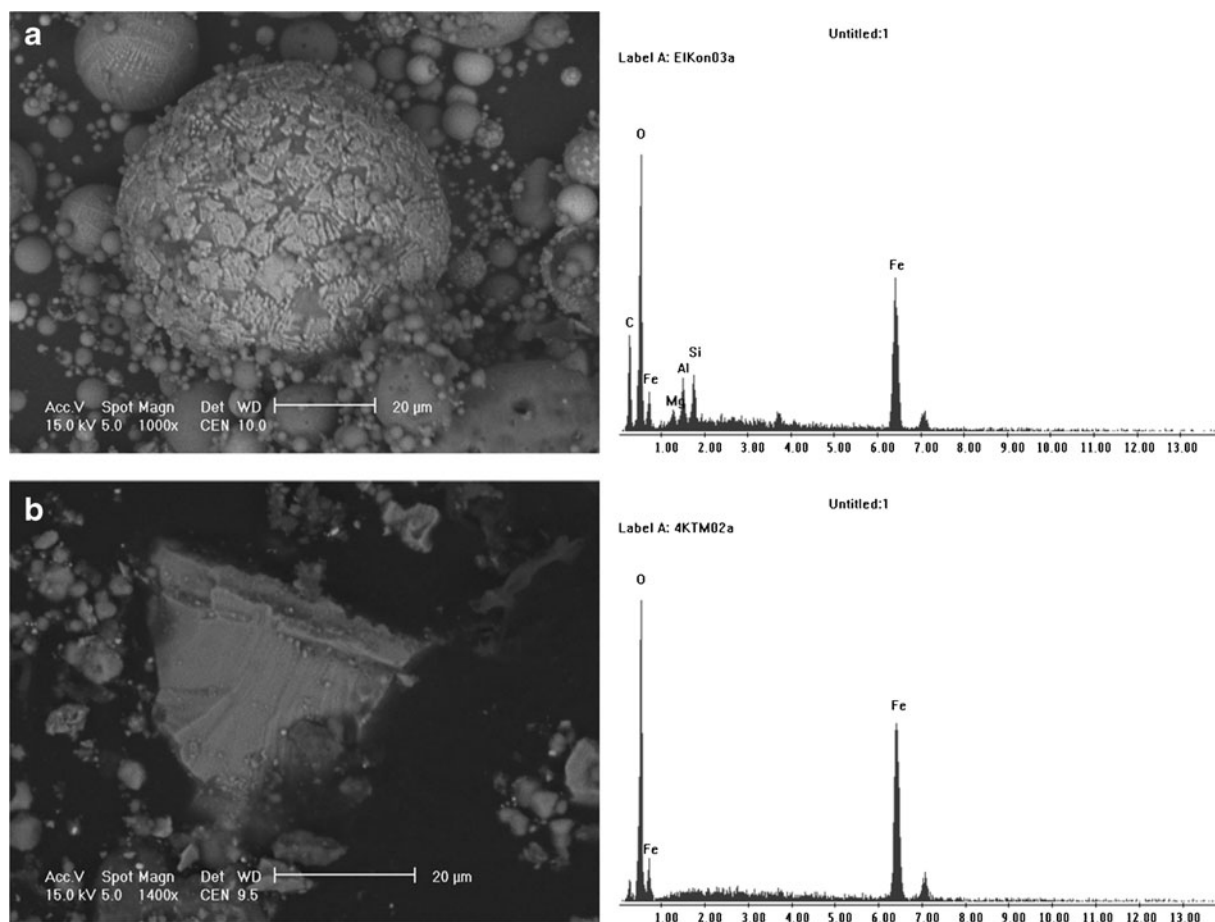


**Fig. 2** SEM micrographs of fly ash from lignite burning power plant with EDS spectra: **a** incrustation of iron oxide on aluminosilicate spherical particle, **b** angular particle of iron oxide

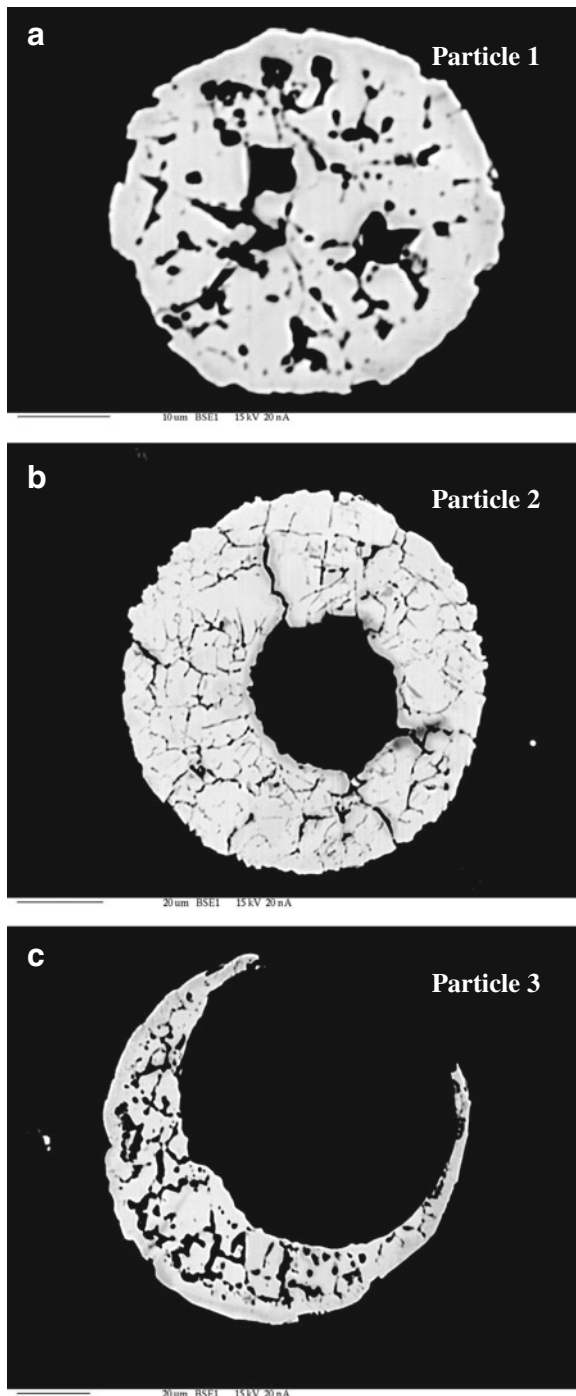


**Fig. 3** Cross-section through the complete (a) and hollow (b and c) magnetic spherules. Pictures taken with the microprobe on magnetic concentrate extracted from fly ash after lignite burning. Chemical composition of these particles is shown in Table 2

crusts with visible holes. These forms were often cracked with a very extensive internal surface which can adsorb heavy metals, as confirmed by stoichiometric analyses (Table 2).

The magnetic fraction of cement dust occurred mostly in the form of angular and octahedral grains of a significantly finer granulation (<20 μm). The oxide forms of iron were commonly found there, in many cases with a considerable admixture of calcium, suggesting calcium ferrites with the chemical composition  $\text{CaFe}_3\text{O}_5$ , rather than pure stoichiometric magnetite (Fig. 4).

Magnetic spherules as well as angular forms were also present. Diphasic structure of spherules was often seen on the cross-sections through magnetic spherules visible in the pictures taken by the microprobe (Fig. 5). Their interior is probably close to the magnetite phase, and the outer zone is made up of maghemite (Table 3).

In the non-magnetic phase, aluminosilicate particles were present with admixtures of iron, sodium, potassium, and magnesium, probably derived from the application of silica-bearing additives, mainly quartz

**Table 2** Stoichiometric analysis of chemical composition of magnetic particles no. 1, 2, and 3 shown in the Fig. 3 occurring in magnetite concentrate extracted from fly ash after lignite combustion

	Particle 1	Particle 2	Particle 3
$\text{P}_2\text{O}_5$	0.006	0.019	0.010
$\text{SiO}_2$	0.087	0.000	0.047
$\text{SO}_2$	0.012	0.000	0.043
$\text{TiO}_2$	0.031	0.021	0.002
$\text{Al}_2\text{O}_3$	0.000	0.037	0.113
$\text{Fe}_2\text{O}_3$	99.731	98.102	100.081
$\text{MgO}$	0.297	0.135	0.582
$\text{CaO}$	0.213	0.041	0.278
$\text{MnO}$	0.000	0.000	0.302
$\text{CoO}$	0.066	0.065	0.038
$\text{NiO}$	0.144	0.032	0.023
$\text{CuO}$	0.000	0.000	0.045
$\text{ZnO}$	0.094	0.000	0.000
$\text{CdO}$	0.048	0.019	0.000
$\text{PbO}$	0.003	0.044	0.000
$\text{Na}_2\text{O}$	0.000	0.011	0.000
Total (%)	100.711	98.526	101.564



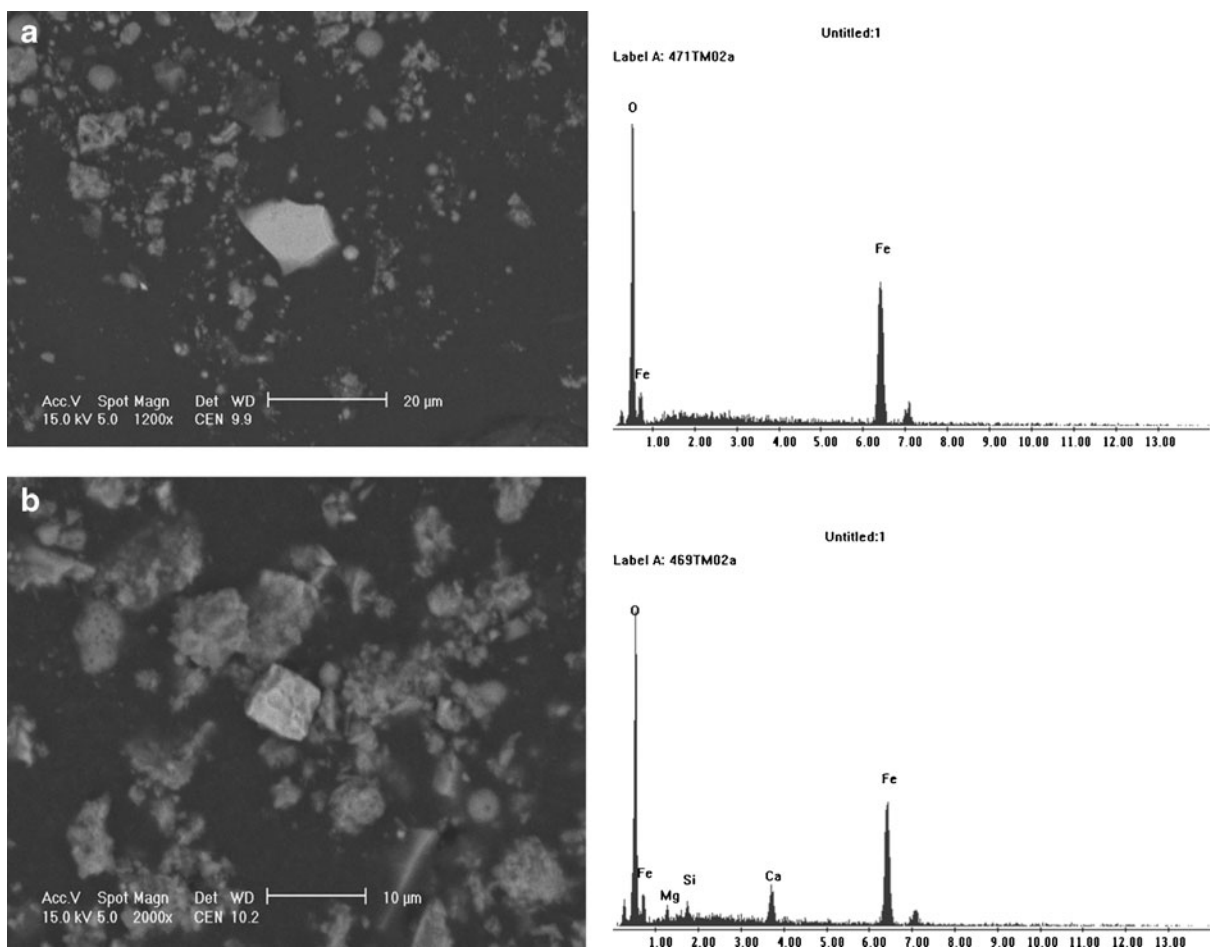


**Fig. 4** SEM micrographs of the magnetic concentrate extracted from cement dust with EDS spectra: **a** irregular magnetite particle in dust falling into the area of cement plant, **b** octahedral

particle of iron oxide (probably calcium ferrite  $\text{CaFe}_3\text{O}_5$ ) in emitted cement dust collected behind electro-filter

sand and waste silica, to the production of clinker in the tested cement plants. They occurred as spherical and irregular, rough or smooth forms of 10 to 20  $\mu\text{m}$  in size. Particles of calcite were also observed in cement dust, probably derived from the use of raw materials for clinker production. Molecules of sylvinite in the shape of irregular forms with a diameter of several microns were also noted, as were slightly larger particles of lead chloride occurring in the forms of angular grains with smooth surfaces and dimensions from 3 to 10  $\mu\text{m}$  (Fig. 6).

Former studies determined diffraction patterns of the magnetite concentrates extracted from samples of ash and cement dust as well as thermomagnetic analyses of ash samples (Magiera et al. 2011). In the case of ash from hard coal burning, these studies show the

dominance of three ferrimagnetic minerals: magnetite, magnesioferrite, and maghemite. Hematite occurs here in much smaller quantities (Fig. 7a). The amount of quartz and mullite, which are physically linked (sintered), was also significant.

Maghemite and hematite are dominant in the magnetic minerals in ash formed from lignite combustion, while strong ferrimagnetic minerals such as magnetite and magnesioferrite occur as subordinate components (Fig. 7b); this explains the much lower magnetic susceptibility of this ash in relation to the ash from hard coal combustion.

The analyses of X-ray diffraction patterns show that—in terms of mineralogical composition—the magnetic fraction in cement dust samples is much more diverse than in the other kinds of tested dust. The

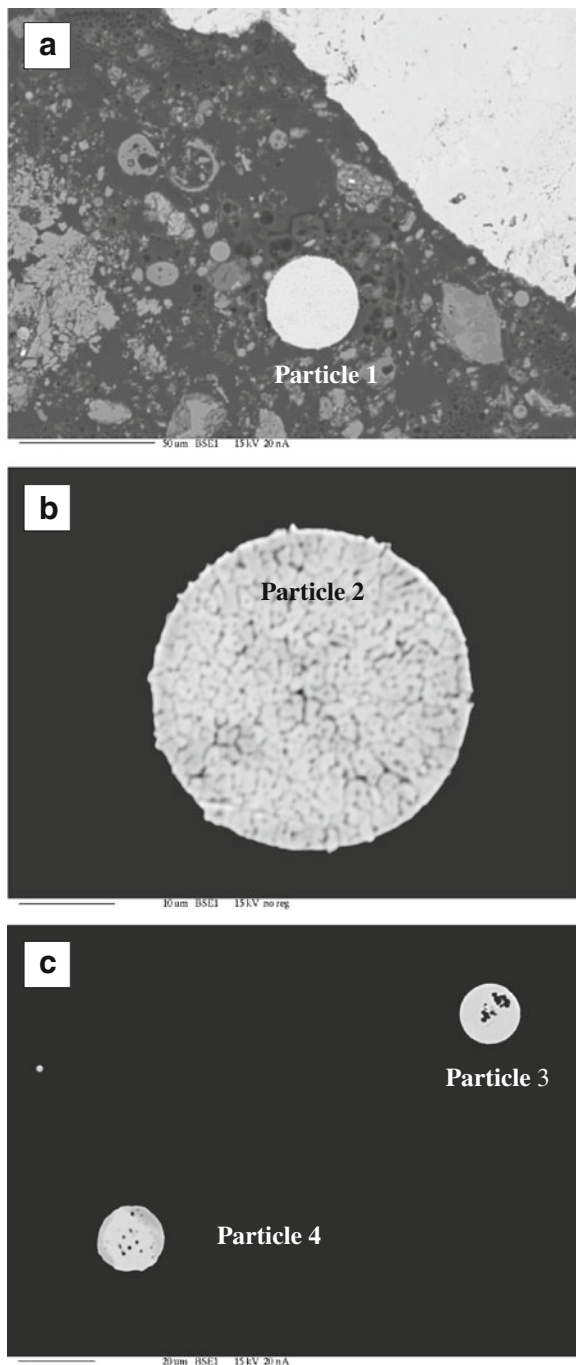


**Fig. 5** Cross-section through the complete spherules. Pictures taken with microprobe on magnetic concentrate of cement dust falling into the area of cement plant. Chemical composition of these particles is shown in Table 3

dominant magnetic minerals here are magnetite, maghemite, and also the forms of ferrites with a significant content of calcium. Other than these dominant

magnetic minerals, hematite and goethite are also present within the magnetic phase. Ferrimagnetic minerals in magnetic concentrates are accompanied by a large amount of diamagnetic minerals, such as anhydrite, calcite, bassanite, gypsum, and quartz (Fig. 7c).

Thermomagnetic analyses performed on fly ash samples showed that the dominant magnetic phase in dust from the combustion of hard coal is magnetite with a specific Curie temperature of  $\sim 580$  °C. During heating of the sample to a temperature of 700 °C, no formation of any other magnetic minerals was noted, and the curves for heating and cooling were almost identical (Fig. 8a). In the case of ash after the burning of lignite, thermomagnetic analyses show that the Curie point is shifted well above a temperature of 600 °C, suggesting the likely presence of significant quantities of maghemite (Curie point ca. 640 °C) or hematite (the Neel temperature of pure hematite is 675 °C). The magnetic susceptibility of the cooling curve was lower than the initial magnetic susceptibility, suggesting that certain parts of magnetite or maghemite were transformed into weakly magnetic forms (Fig. 8b).

Thermomagnetic curves of cement dust measured during this study (only those with a value of  $\chi$  above  $50 \times 10^{-8} \text{ m}^3 \text{ kg}^{-1}$  were subjected to thermomagnetic studies) were more diverse, but in all tested samples the dominance of magnetite as the main magnetic mineral was clearly marked, occurring most often within a fairly wide range of particle size. In most tested samples, the presence of hematite also cannot be excluded (Fig. 9). Sometimes there were also rises in magnetic susceptibility at temperatures above 300 °C, suggesting the presence of sulfides. In some samples of cement dust, two magnetic phases clearly appeared on the cooling curve (at a temperature of 450 and 550 °C). For the majority of cement dust samples, the cooling curves were above the heating curves, and the magnetic susceptibility after thermal treatment was two to four times higher than at the beginning. This suggests the transition of weakly magnetic mineral phases into ferrimagnetic forms, which presumably means that, during the heating of the sample, secondary magnetite occurs.

A comparison of all mineral forms of alkaline dust identified in the tested samples is presented in Table 4. The basic components of dust samples from hard coal combustion in power plants are amorphous substance

**Table 3** Stoichiometric analysis of the chemical composition of spherical particles no. 1, 2, 3, and 4, shown in Fig. 5, occurring in magnetic concentrate extracted from cement dust

	Particle 1	Particle 2	Particle 3	Particle 4
P <sub>2</sub> O <sub>5</sub>	0.031	0.000	0.057	0.002
SiO <sub>2</sub>	1.115	1.501	1.867	0.061
SO <sub>2</sub>	0.018	0.022	0.116	0.014
TiO <sub>2</sub>	0.020	0.033	0.677	0.031
Al <sub>2</sub> O <sub>3</sub>	1.330	1.339	2.207	0.248
Fe <sub>2</sub> O <sub>3</sub>	97.931	98.167	67.791	100.353
MgO	0.378	0.391	0.604	0.430
CaO	0.225	0.314	22.251	0.073
MnO	0.093	0.081	0.243	0.074
CoO	0.000	0.059	0.038	0.028
NiO	0.003	0.047	0.033	0.000
CuO	0.000	0.000	0.000	0.000
ZnO	0.000	0.020	0.000	0.000
CdO	0.000	0.000	0.017	0.000
PbO	0.111	0.000	0.064	0.000
Na <sub>2</sub> O	0.038	0.016	0.041	0.000
Total (%)	101.332	101.990	95.506	101.320

(glassy phase; ~40 % vol.) and mullite (~15 %), with a slightly lower amount of magnesioferrite/magnetite with hematite ( $\Sigma$ ~12 %), quartz (~10 %), MgO in the form of periclase (~8 %), probably the Ca-Mg silicate (smectite), lime CaO, and a trace content of anhydrite.

The phase composition of dust samples after lignite burning in power plants include anhydrite (~25 % vol.), maghemite with hematite and magnetite ( $\Sigma$ ~20 %), CaO (~12 %), MgO (~10 %), portlandite, quartz, the Ca<sub>3</sub>Al<sub>6</sub>O<sub>12</sub>·CaSO<sub>4</sub> phase, merwinite, the intermediate member of the akermanite-gehlenite series, and the admixture of bassanite and mullite. Difficult-to-determine calcium silicate is also present (reflex~9.3–9.4 Å).

Three main substances occurred in the mineral composition of cement dust: anhydrite with bassanite ( $\Sigma$ ~32 %), and calcite (~28 %). Smaller amounts were found of: hematite with magnetite and goethite ( $\Sigma$ ~15 %), sylvinitic and/or CaSO<sub>4</sub>, ammoniojarosite, quartz, kaolinite, illite, and ettringite.

#### 4 Discussion

Recognition of the morphological and mineralogical features of alkaline dust, especially the magnetic

fraction contained therein, is essential to reveal the magnetic properties of iron minerals as indicators of soil pollution caused by the deposition of industrial dust, including fly ash, onto the soil. The performed analyses confirmed the presence of a considerable amount of technogenic magnetic particles in alkaline dust. The easily measurable value of magnetic susceptibility is directly proportional to the content of these particles in the measured sample and can be used to estimate the anthropogenic dust content in topsoil. The tested dust showed different values of  $\chi$ , mostly dependent on the type of coal, the temperature and conditions of combustion in power boilers, the type of raw materials, additives and fuels used for cement and lime production, the size of their consumption, as well as the manufacturing method for cement and lime.

The highest value of magnetic susceptibility was shown by the fly ash samples from the combustion of hard coal. This is caused by the high temperature of the combustion resulting in a high content of ferrimagnetic minerals. The major source of iron in hard coal is framboidal pyrite. At the temperatures of coal combustion, the conversion of weakly magnetic sulfides (pyrite and marcasite) into the ferrimagnetic forms of iron oxides (magnetite and maghemite) takes place (Mitchell and Gluskoter 1976; Lauf et al. 1982). The creation of maghemite was observed within the

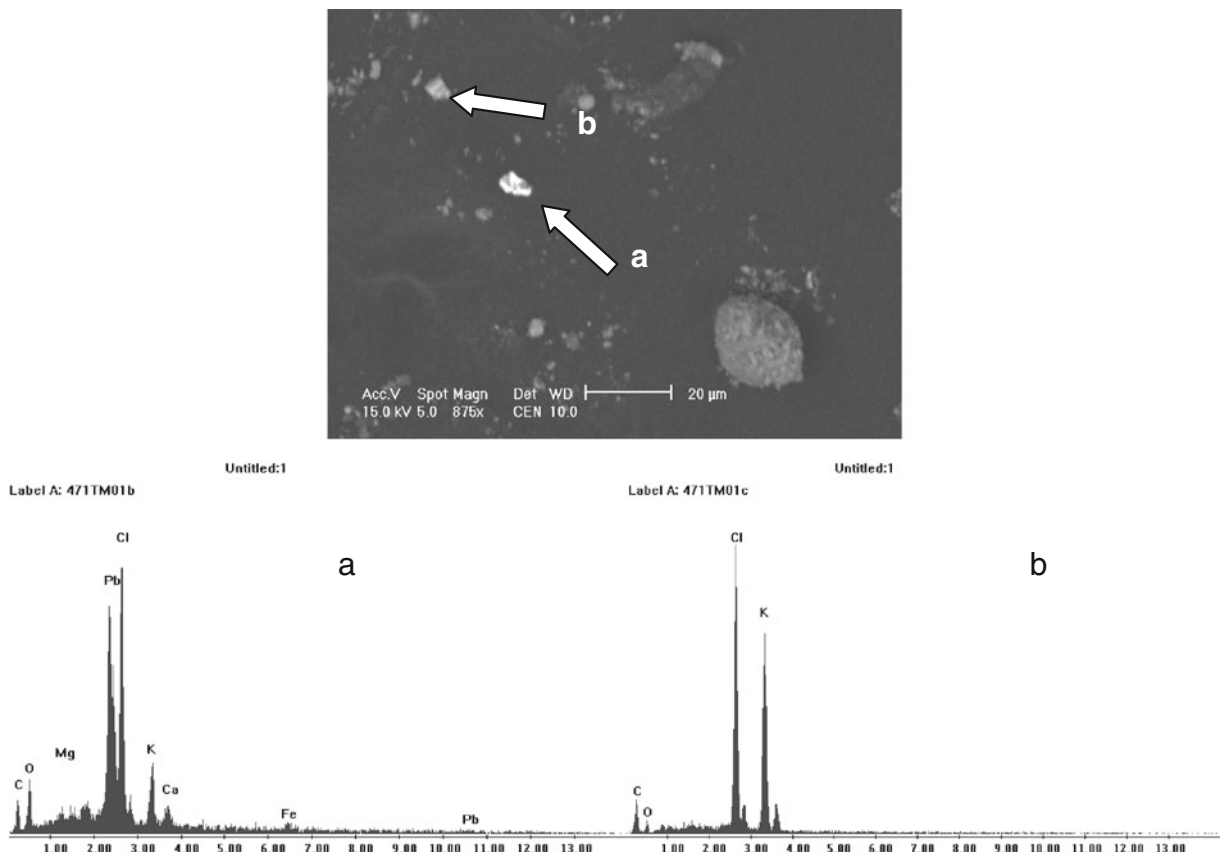


**Fig. 6** SEM micrographs of lead chloride (a) and sylvinite (b) with EDS spectra–cement dustfall

temperature range of 800–1,400 °C and magnetite 1,300–1,600 °C. Some authors also suggest that, at a temperature approximately 550 °C, the dissociation of pyrite occurs, resulting in conversion to troilite via ferrimagnetic pyrrhotite (Gryglewicz et al. 1996; Gupta et al. 2007).

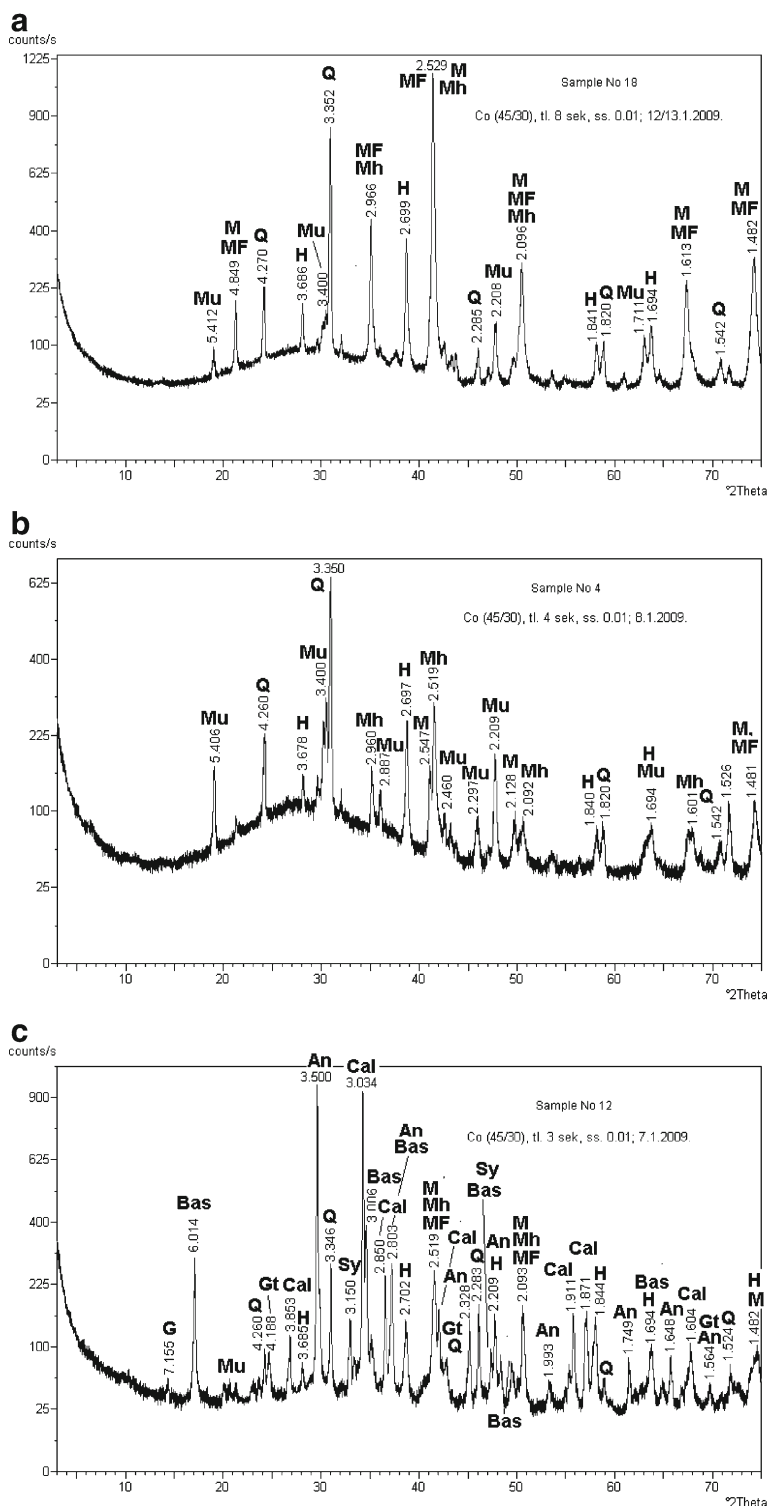
The ease with which pyrite undergoes dissociation and oxidation makes it a particularly significant substrate in the high-temperature processes of the formation of ferrimagnetic minerals. Pyrite is one of the most important iron minerals present in coal, with a content reaching 15 %.

Fly ash from the combustion of lignite showed slightly lower but also high values of magnetic susceptibility, with a maximum average value of  $\chi$  reaching  $590 \times 10^{-8} \text{ m}^3 \text{ kg}^{-1}$ . The results of qualitative analysis and scanning electron microscopy confirmed the high content of ferrimagnetic minerals in dusts from power plants. In fly ash from hard coal combustion, the content of magnesioferrite/magnetite phase together with hematite was ~12 %, and from lignite

combustion the contribution of magnetite or maghemite with hematite was ~20 %. In the case of fly ash from hard coal, ferrimagnetic magnesioferrite/magnetite minerals were predominant among TMPs, whereas in the case of ash from lignite combustion a considerable amount of maghemite (which is also ferrimagnetic, but with a lower spontaneous magnetization) and/or antiferromagnetic hematite was observed. Iron oxides in the analyzed fly ash samples occurred in the specific morphological form of magnetic spherules with a grain size of 20–50 μm, but there were also a considerable number of grains smaller than 10 μm.

Cement dust was much more diverse, both magnetically and mineralogically. The X-ray phase analysis and SEM analysis also confirmed the participation of magnetic particles in cement dust. The results of the study showed that the values of  $\chi$  of cement dust samples are highly variable. For some kinds of dust it was above  $800 \times 10^{-8} \text{ m}^3 \text{ kg}^{-1}$ , providing a high content of ferrimagnetic minerals and, in other cases, mainly in the dust from lime plants, it had a value of

**Fig. 7** X-ray diffraction pattern of the following samples: **a** fly ash from hard coal burning, **b** fly ash from lignite burning, **c** cement dust. *Mh* maghemite, *MF* magnesioferrite, *M* magnetite, *H* hematite, *Mu* mullite, *Q* quartz, *Gt* goethite, *An* anhydrite, *Cal* calcium, *Bas* bassanite, *G* gypsum (Magiera et al. 2011)

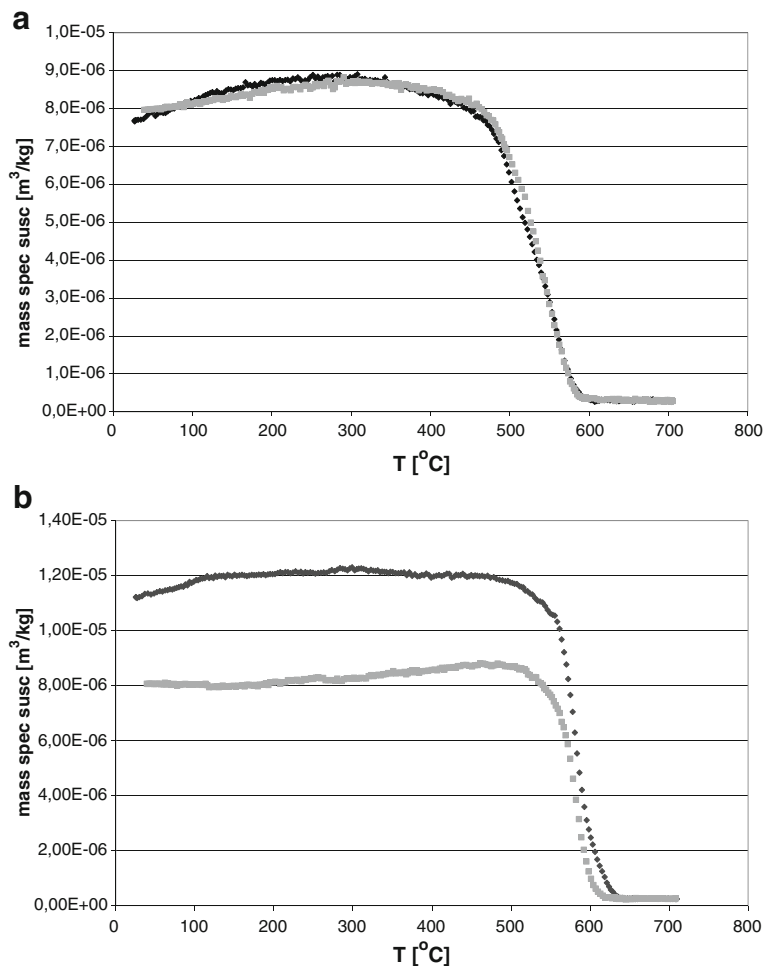


$1$  or  $2 \times 10^{-8} \text{ m}^3 \text{ kg}^{-1}$ , which is at the level of diamagnetic or paramagnetic minerals, confirming a marginal content of iron minerals in the samples.

As proved during earlier studies (Gołuchowska and Strzyszc 1999; Gołuchowska 2001), the sources of magnetite in cement dust are raw materials and



**Fig. 8** Thermomagnetic curves of two samples of fly ash emitted by power plant: **a** hard coal burning, **b** lignite burning. *Black* heating line, *grey* cooling line (Magiera et al. 2011)



additives used in cement production and ash from the combustion of hard coal in cement kilns. Iron-bearing additives have the greatest impact on the magnetic susceptibility of cement dust and should be considered the most dangerous to the environment.

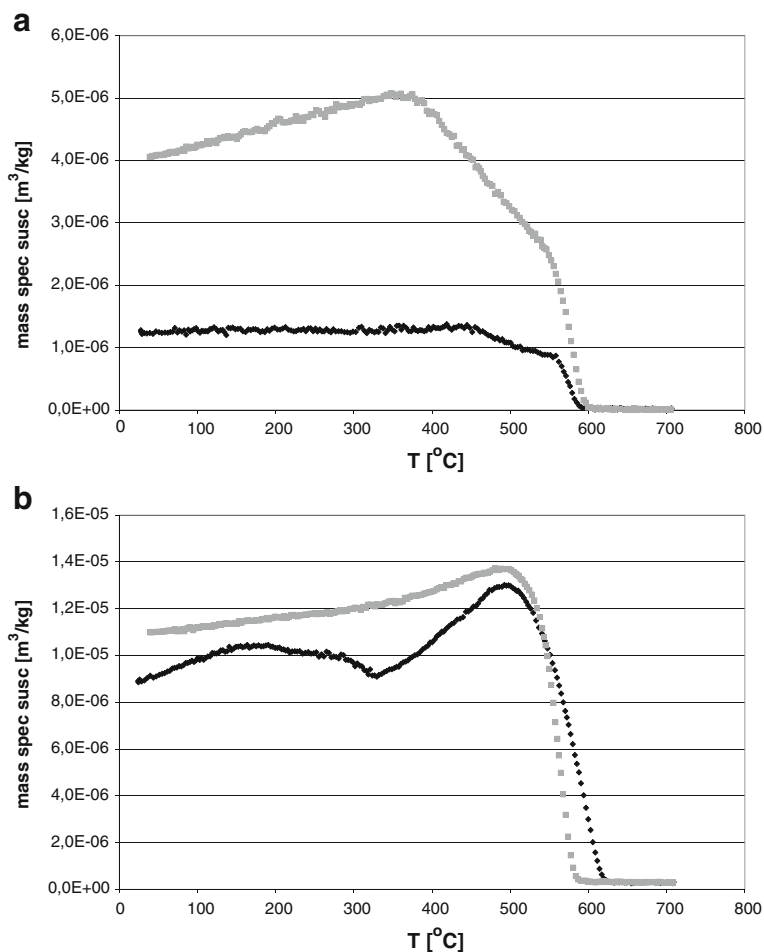
The lowest values of magnetic susceptibility are characteristic of alkaline dust from lime plants, which contains mostly diamagnetic and paramagnetic substances. This may be related to the fact that—compared with cement production—lime production technology does not use corrective additives, the so-called low raw materials such as marl, clay etc., as well as coal to fire lime kilns.

The research into TMPs in atmospheric dust collected in Upper Silesia (Southern Poland) has shown that most of the magnetic particles have a spherical shape, characteristic of particles produced in the processes of solid fuel (hard coal) combustion (Strzyszc

1993; Magiera et al. 2002; Magiera et al. 2010). These are called magnetic spherules and their size varies from a few to several dozen micrometers. Some have a smooth surface, others are corrugated, and some are fused with the silicate phase (mainly the mullite or glassy phase).

The internal structure of the spherules is twofold. Some spheres, having a smaller diameter, are solid and consist of a magnetic core consisting of non-stoichiometric spinel of a magnetite–maghemite series ( $\text{Fe}_{3-x}\text{Me}_x\text{O}_4$ ), or a mineral with the structure of ferrite ( $\text{MeFe}_2\text{O}_4$ ) (Hullet et al. 1980; Strzyszc et al. 1996). They are usually surrounded by a thin silicate, aluminosilicate, or calcareous coating. The magnetic spherules of the second type are hollow, and their shell is mainly composed of magnetite or an intermediate phase of magnetite–maghemite. There are visible holes on the surface of the latter, being the outlets of

**Fig. 9** Thermomagnetic curves of two cement dust samples collected from chimney electrofilters (**a**—zone I, **b**—zone II). *Black*—heating line, *grey*—cooling line



the gas. These were formed during rapid solidification of iron oxides and silica at high temperature, as evidenced by the significant amounts of silicate glassy phase and mullite.

The results of the study showed that technogenic magnetic particles, being a carrier of magnetic signals in atmospheric dust, often also contain significant amounts of elements, including heavy metals (Mn, Zn, and Ni; Tables 2 and 3). They can be bound either in a spinel crystalline structure, or by the forces of surface adsorption. In the latter case, after deposition on the soil surface, particularly in forest areas where soils are usually acidic, they may be relatively easily released into the environment, posing a potential ecological threat.

The analysis of the results of SEM-EDS studies showed that there are differences in the kinds of metals associated with magnetic particles at the different sampling sites. In the area of Dąbrowa Górnicza–Łosień

(Upper Silesia, Southern Poland), situated in the direct range of the influence of the “Katowice” Steelworks, and especially in the area of Siemianowice–Michałkowice, in close proximity to “Jedność” Steelworks, and a few other old steelworks of the central part of the Upper Silesian Industrial Region, a relationship between magnetic particles and nickel and chromium was found, these being the specific metals associated with the iron and steel industry. A greater quantity of angular particles was also observed in the atmospheric dust in this area. Their presence in soil organic levels had previously been reported in the areas of ferrous metallurgy, particularly near the old steel plants (Magiera et al. 2002; 2008). Atmospheric dust samples collected in these areas clearly showed the highest  $\chi$  value. This was not only a result of the largest accumulation of ferrimagnetic iron oxides, but also the presence of metallic iron ( $\alpha$  Fe), which occurred in the form of angular particles. Metallic iron is the strongest ferromagnet and its magnetic susceptibility is approximately 400 times higher

**Table 4** Mineral phases identified in alkaline dust samples

Mineralogical composition of alkaline dust samples		
Power plant dusts—from hard coal combustion	Power plant dusts—from lignite combustion	Cement dust
Mullite $3\text{Al}_2\text{O}_3 \times 2\text{SiO}_2$	Anhydrite $\text{CaSO}_4$	Bassanite $\text{CaSO}_4 \times 0.5\text{H}_2\text{O}$
Magnetite $\text{FeFe}_2\text{O}_4$	Hematite $\alpha\text{-Fe}_2\text{O}_3$	Anhydrite $\text{CaSO}_4$
Magnesian ferrite $\text{MgFe}_2\text{O}_4$	Maghemite $\beta\text{-Fe}_2\text{O}_3$	Calcite $\text{CaCO}_3$
Hematite $\alpha\text{-Fe}_2\text{O}_3$	Magnetite $\text{FeFe}_2\text{O}_4$	Hematite $\alpha\text{-Fe}_2\text{O}_3$
Quartz $\text{SiO}_2$	Lime $\text{CaO}$	Magnetite $\text{FeFe}_2\text{O}_4$
Periclase $\text{MgO}$	Periclase $\text{MgO}$	Ca-ferrite $\text{CaFe}_3\text{O}_5$
Lime $\text{CaO}$	Portlandite $\text{Ca}[\text{OH}]_2$	Goethite $\alpha\text{-FeOOH} - \beta\text{-FeOOH}$
Smectite	Quartz $\text{SiO}_2$	Anthropogenic calcium sulfate $\text{CaSO}_4$
$\text{M}_x(\text{Al}_{1.67}\text{Mg}_{0.33})[\text{Si}_4\text{O}_{10}](\text{OH})_2$	$\text{Ca}_3\text{Al}_6\text{O}_{12} \times \text{CaSO}_4$ phase	Sylvinitic KCl
Anhydrite $\text{CaSO}_4$	Merwinite $\text{Ca}_3\text{Mg}[\text{SiO}_4]_2$	Ammoniojarosite $(\text{NH}_4)\text{Fe}_3[\text{SO}_4]_2(\text{OH})_6$
	Akermanite $\text{Ca}_2\text{Mg}[\text{Si}_2\text{O}_7]$ —gehlenite $\text{Ca}_2\text{Al}[(\text{Al}, \text{Si})_2\text{O}_7]$	Quartz $\text{SiO}_2$
	Bassanite $\text{CaSO}_4 \times 0.5\text{H}_2\text{O}$	Kaolinite $\text{Al}_4[\text{Si}_4\text{O}_{10}](\text{OH})_8$
	Mullite $3\text{Al}_2\text{O}_3 \times 2\text{SiO}_2$	Illite $(\text{K}_9\text{H}_3\text{O}^+)\text{Al}_2[\text{AlSi}_3\text{O}_{10}](\text{OH})_2$
	Calcium silicate $\text{CaO} \times \text{SiO}_2$	Ettringite $\text{Ca}_6\text{Al}_2[\text{SO}_4(\text{OH})_4]_3 \times 24 \text{H}_2\text{O}$

than the magnetic susceptibility of the stoichiometric magnetite (Thompson and Oldfield 1986).

Magnetic particles present in dust falling onto the soil surface may cause an increase in the magnetic susceptibility of the upper soil horizons (Kusza and Strzyszc 2005). According to Strzyszc (1993), magnetite content in soils in the immediate vicinity of industrial plants is high. Furthermore, the increase in magnetic susceptibility of the soil covered by alkaline dust emissions is a result of the enrichment of soil in iron oxides, which may act as carriers of heavy metals. Zawadzki et al. (2004) confirms a high correlation between the rise in magnetic susceptibility and the increased content of heavy metals in industrial dust. In the case of cement dust, high correlation coefficients with magnetic susceptibility were observed for the following metals: iron, manganese, lead, and cadmium and, in the case of fly ash, for iron, manganese, zinc, and lead.

Taking into account the significant correlation between industrial emissions and increased magnetic susceptibility of the soil, and the fact that magnetic particles can be carriers of heavy metals, methods for magnetic measurement should be considered as

particularly useful in monitoring the state of the soil environment.

## 5 Conclusions

- Alkaline dust released into the atmosphere from coal combustion and cement production processes and deposited in the topsoil have pH values between 8 and 12. They contain technogenic magnetic particles that can be used as an easily measurable tracer of this kind of pollution.
- In fly ash from coal burning power plants, TMPs occur in very characteristic spherical forms of various sizes from several to dozens of micrometers, the so-called magnetic spherules. Ferrimagnetic iron oxides (magnetite and maghemite) frequently form incrustation on the surface of mullite, amorphous silica, or aluminosilicate particles. Other spherules consist entirely of a ferrimagnetic shell built of iron oxide, and their inside is void with visible holes after gas escape.
- In fly ash from lignite combustion, maghemite and hematite prevail while strong ferrimagnetic

minerals such as magnetite and magnesioferrite occur as a minor fraction, which explains the much lower magnetic susceptibility of this ash in comparison with the ash from hard coal combustion.

- The mineralogical nature of TMPs in cement dust is more diverse. The magnetic fraction of cement dust occurs mostly in the form of angular and octahedral grains of a significantly finer granulation (<20 µm). In many cases, ferrimagnetic minerals occur here with a considerable admixture of calcium. Sometimes they form calcium ferrites (CaFe<sub>3</sub>O<sub>5</sub>), rather than pure stoichiometric magnetite or maghemite. Iron-bearing additives have the greatest impact on the magnetic susceptibility of cement dust, and should be considered the most dangerous to the environment.
- Stoichiometric analyses confirmed the presence of heavy metals such as Pb, Mn, Cd, and Zn connected with TMPs, which are carriers of a magnetic signal in atmospheric dust, and therefore in some cases their presence in topsoil detected by magnetic measurement can be treated as an indicator of inorganic soil contamination.

**Acknowledgments** We thank Dr Aleš Kapička from the Institute of Geophysics, Academy of Sciences of the Czech Republic for help with thermomagnetic analysis and data interpretation and also Dr Grażyna Bzowska for X-ray analysis. Many thanks to professional Proof-Reading-Service for detailed proofreading of the article.

**Open Access** This article is distributed under the terms of the Creative Commons Attribution License which permits any use, distribution, and reproduction in any medium, provided the original author(s) and the source are credited.

## References

Beckwith, P. R., Ellis, J. B., Revitt, D. M., & Oldfield, F. (1986). Heavy metal and magnetic relationships for urban source sediments. *Physics of The Earth and Planetary Interiors*, 42(1–2), 67–75.

Farmer, A. M. (1993). The effects of dust on vegetation—a review. *Environmental Pollution*, 79, 63–75.

Giere, R., & Querol, X. (2010). Solid particulate matter in the atmosphere. *Elements*, 6, 215–222.

Gołuchowska, B. J. (2001). Some factors affecting an increase in magnetic susceptibility of cement dusts. *Journal of Applied Geophysics*, 48, 103–112.

Gołuchowska, B., & Strzyszczyński, Z. (1999). The influence of clinker technology on heavy metal content in dusts

generated in the process of clinker burning. *Ecological Chemistry and Engineering*, 6, 217–227 (in Polish).

Gryglewicz, G., Wilk, P., Yperman, J., Franco, D. V., Meas, I. I., Mullens, J., & van Poucke, L. C. (1996). Interaction of the organic matrix with pyrite during pyrolysis of high-sulphur bituminous coal. *Fuel*, 75, 1499–1504.

Gupta, S., Dubikova, M., French, D., & Sahajwalla, V. (2007). Characterization of the origin and distribution of the minerals and phases in metallurgical cokes. *Energy & Fuels*, 21, 303–313.

Hansen, L. D., Silberman, D., & Fisher, G. L. (1981). Crystalline components of stack collected, size-fractionated coal fly ash. *Environmental Science & Technology*, 15, 1057–1062.

Hullet, L. D., Weinberger, A. J., Northcutt, K. J., & Ferguson, M. (1980). Chemical species in fly ash from coal-burning power plant. *Science*, 210, 1356–1358.

Hunt, A., Jones, J., & Oldfield, F. (1984). Magnetic measurements and heavy metals in atmospheric particulates of anthropogenic origin. *Science of the Total Environment*, 33, 129–139.

Keyser, T. R., Natush, C. A., Evans, C. A., Jr., & Linton, R. W. (1978). Characterizing the surfaces of environmental particles. *Environmental Science & Technology*, 12, 768–773.

Klose, S., Koch, J., Bäuker, E., & Makeschin, F. (2001). Indicative properties of fly-ash affected forest soils in North-eastern Germany. *Journal for Plant Nutrition & Soil Science*, 164, 561–568.

Koniecznyński, J., & Stec, K. (2009). The occurrence of selected trace elements in grain fractions of dust emitted from power, coke and cement plants. *Archives of Environmental Protection*, 35(4), 3–21.

Koniecznyński, J., & Zeliński, J. (2009). Fractional composition of dust emitted from boilers with circulating fluidized beds. *Archives of Environmental Protection*, 35(1), 3–11.

Koniecznyński, J., Komosiński, B., & Zelechower, M. (2007). Properties of particulate matter emitted from manufacturing of ceramic products. *Archives of Environmental Protection*, 33, 3–22.

Kusza, G., & Strzyszczyński, Z. (2005). Forest reserves of Opole Province—state and technogenic hazards. Institute of Environmental Engineering of the Polish Academy of Sciences, Zabrze. *Works & Studies No.*, 63, 1–156 (in Polish).

Lauf, R. J., Harris, L. A., & Rawiston, S. S. (1982). Pyrite framboids as the source of magnetite spheres in fly ash. *Environmental Science & Technology*, 16, 218–220.

Magiera, T., Lis, J., Nawrocki, J., & Strzyszczyński, Z. (2002). *Magnetic susceptibility of soils in Poland* (pp. 1–6). Warsaw: National Geological Institute. (in Polish).

Magiera, T., Kapička, A., Petrovský, E., Strzyszczyński, Z., Fialová, H., & Rachwał, M. (2008). Magnetic anomalies of forest soils in the Upper Silesia-Northern Moravia region. *Environmental Pollution*, 156, 618–627.

Magiera, T., Strzyszczyński, Z., Jabłońska, M., & Bzowska, G. (2010). Characterization of magnetic particulates in urban and industrial dusts. In C.A., Brebbia & J.W.S., Longhurst (Eds.), *Air Pollution XVIII. Transactions on Ecology and the Environment ed., Vol. 136*, (pp. 171–184) WIT Press.

Magiera, T., Jabłońska, M., Strzyszczyński, Z., & Rachwał, M. (2011). Morphological and mineralogical forms of

- technogenic magnetic particles in industrial dusts. *Atmospheric Environment*, 45, 4281–4290.
- Migaszewski, Z. M., Gałuszka, A., Świercz, A., & Kucharzyk, J. (2001). Element concentrations in soils and plant bio-indicators in selected habitats of the Holy Cross Mts., Poland. *Water, Air, and Soil Pollution*, 129, 369–386.
- Mitchell, R. S., & Gluskoter, H. J. (1976). Mineralogy of ash of some American coals: variations with temperature and source. *Fuel*, 55, 90–96.
- Polat, R., Gürol, A., Budak, G., Karabulut, A., & Ertuğrul, M. (2004). Elemental composition of cement kiln dust, raw material and cement from a coal-fired cement factory using energy dispersive X-ray fluorescence spectroscopy. *Journal of Quantitative Spectroscopy and Radiative Transfer*, 83(3–4), 377–385.
- Puffer, J. H., Russell, E. W. B., & Rampino, M. R. (1980). Distribution and origin of magnetite spherules in air, water and sediments of the greater New York City area and the north Atlantic Ocean. *Journal of Sedimentary Research*, 50, 247–256.
- Sagnotti, L., Taddeucci, J., Winkler, A., & Cavallo, A. (2009). Compositional, morphological, and hysteresis characterization of magnetic airborne particulate matter in Rome, Italy. *Geochemistry, Geophysics, Geosystems*, 10, 1–17.
- Strzyszczyk, Z. (1993). Magnetic susceptibility of soils in the area influenced by industrial emissions. In *Soil Monitoring, Monte Verita*, Birkhäuser Verlag, Basel, 255–269.
- Strzyszczyk, Z. (1995). Gehalt an Ferromagnetika in den von der Immision der Zementindustrie in der Wojewodschaft Opole beeinflussten Böden. *Mitteilungen der Bodenkundlichen Gesellschaft*, 76, 1477–1480.
- Strzyszczyk, Z., & Magiera, T. (1998). Heavy metal contamination and magnetic susceptibility in soils of Southern Poland. *Physics and Chemistry of the Earth*, 23, 1127–1131.
- Strzyszczyk, Z., Magiera, T., & Heller, F. (1996). The influence of industrial emissions on the magnetic susceptibility of soils in Upper Silesia. *Studia geophysica et geodaetica*, 40, 276–286.
- Thompson, R., & Oldfield, F. (1986). *Environmental magnetism* (pp. 1–227). London: Allen and Unwin.
- Vassilev, S. V., Eskenazy, G. M., & Vassileva, C. G. (2001). Behaviour of elements and minerals during preparation and combustion of the Pernik coal, Bulgaria. *Fuel Processing Technology*, 72, 103–129.
- Vassilev, S. V., Menendez, R., Borrego, A. G., Diaz-Somoano, M., & Martinez-Tarazona, M. R. (2004). Phase-mineral and chemical composition of coal fly ashes as a basis for their multicomponent utilization. 3. Characterization of magnetic and char concentrates. *Fuel*, 83, 1563–1583.
- Vaughan, D. J., Patrick, R. A. D., & Wogelius, R. A. (2002). Minerals, metals and molecules: ore and environmental mineralogy in the new millennium. *Mineralogical Magazine*, 66(5), 653–676.
- Zawadzki, J., Magiera, T., & Strzyszczyk, Z. (2004). Correlation and regression analysis of heavy metal content and magnetic susceptibility in soils from Upper Silesian Industrial Region. *Archives of Environmental Protection*, 30, 71–82 (in Polish).